

10-1-1996

The ^9Be Abundances of alpha Centauri A and B and the Sun: Implications for Stellar Evolution and Mixing

Jeremy R. King

Clemson University, jking2@clemson.edu

Constantine P. Deliyannis

Yale University

Ann Merchant Boesgaard

University of Hawaii

Follow this and additional works at: https://tigerprints.clemson.edu/physastro_pubs

Recommended Citation

Please use publisher's recommended citation.

This Article is brought to you for free and open access by the Physics and Astronomy at TigerPrints. It has been accepted for inclusion in Publications by an authorized administrator of TigerPrints. For more information, please contact kokeefe@clemson.edu.

THE ${}^9\text{Be}$ ABUNDANCES OF α CENTAURI A AND B AND THE SUN: IMPLICATIONS FOR STELLAR EVOLUTION AND MIXING

JEREMY R. KING^{1,2}

Department of Astronomy, RLM 15.308, University of Texas, Austin, TX 78712-1083; king@verdi.as.utexas.edu

CONSTANTINE P. DELIYANNIS^{1,2,3}

Department of Astronomy, Center for Solar and Space Research, and Center for Theoretical Physics, Yale University, P.O. Box 208101, New Haven, CT 06520-8101; con@athena.astro.yale.edu

AND

ANN MERCHANT BOESGAARD²

Institute for Astronomy, University of Hawaii at Mānoa, 2680 Woodlawn Drive, Honolulu, HI 96822; boes@galileo.ifa.hawaii.edu

Received 1996 March 29; accepted 1996 October 24

ABSTRACT

We present high-resolution, high signal-to-noise ratio spectra, obtained at the Cerro Tololo Inter-American Observatory 4 m telescope, of the Be II 3131 Å region in the metal-rich solar analog α Centauri A and its companion α Centauri B. Be abundances are derived relative to the Sun in a consistent fashion via spectrum synthesis. For α Cen A, we find $[\text{Be}/\text{H}] = +0.20 \pm 0.15$, where the error reflects random uncertainties at the 1σ confidence level; systematic errors of ~ 0.1 dex are also possible. The analysis of α Cen B is more uncertain since inadequacies in the line list, which was calibrated with solar data, may manifest themselves in cool metal-rich dwarfs. Our analysis suggests $[\text{Be}/\text{H}] \lesssim +0.05$, which is lower than the value of A, but not significantly so given the uncertainties in the A determination alone. In order to derive a conservatively probable and larger extreme range for the solar photospheric Be abundance, we consider various uncertainties (including those in the gf -values, continuum location, non-LTE effects, model atmospheres, analysis codes, and contaminating blends) in its determination. We conclude that the probable range of depletion of photospheric Be from the meteoritic value is 0.16–0.50 dex. Our larger extreme range is 0.05–0.62 dex. Even a slight real depletion in solar photospheric Be itself would strongly contradict the standard solar model (as does the Sun's Li depletion), suggesting the action of additional mechanisms. When coupled with the solar Li depletion of only ~ 2 dex, Be depletion would point to mixing mechanisms (possibly rotationally induced) below the surface convection zone acting on a timescale that is much longer than the convective timescale. If the difference in the Be abundances of α Cen A and B is real, it too would strongly suggest the action of additional mixing mechanisms. The study of both stars with higher resolution data and improved atomic and molecular data is clearly important. We conclude that the light-element abundances of the Sun and α Cen A (and other solar analogs) are not grossly dissimilar. The idea that standard models and the current solar photospheric Li and Be abundance are discrepant because the Sun is a lone “oddball” is doubtful. We also have considered the issue of the unidentified blending feature(s) in the Be II 3131.065 Å region. While a putative Mn I λ 3131.037 feature has several favorable characteristics, we suggest that a single significant blending feature likely lies ~ 0.02 Å blueward of this position.

Subject headings: stars: abundances — stars: individual (α Centauri A, α Centauri B)

1. INTRODUCTION

The photospheric abundances of the light elements Li, Be, and B provide important clues about stellar structure and evolution, as they are destroyed by (p, α)-reactions at temperatures exceeding a few million degrees. The solar Li abundance is roughly a factor of 200 below the meteoritic abundance (e.g., Anders & Grevesse 1989). A definitive explanation for this difference has been elusive for decades, in part because evolutionary solar model convection zones do not attain the required depth for a sufficiently long time to destroy enough Li. Some limited evidence exists that the solar Be abundance may also be depleted, perhaps by as

much as a factor of 2–3. If true, slow mixing below the convection zone would be favored to deplete both Li and Be (though not catastrophically for Li), and this could have wide-ranging implications in astronomy. We emphasize that even though the standard solar models have enjoyed tremendous success recently in terms of agreement between the predicted outer structure and the results from helioseismology (including the depth of the convection zone [e.g., Chaboyer, Demarque, & Pinsonneault 1995; Bahcall & Pinsonneault 1992; Christensen-Dalsgaard, Gough, & Thompson 1991; and references therein]), some observed properties of the Sun still defy explanation, such as the degree of Li depletion, and possibly (if real) Be depletion. These suggest that a fuller understanding of the Sun (and perhaps stars in general) requires the consideration of additional physics beyond that included in standard solar models, possibly such as rotationally induced mixing.

Before drawing general conclusions, it is important to ascertain whether or not the Sun's light-element abun-

¹ Hubble Fellow.

² Visiting Astronomer at the Cerro Tololo Inter-American Observatory, National Optical Astronomy Observatories, operated by the Association of Universities for Research in Astronomy, Inc. (AURA), under a cooperative agreement with the National Science Foundation.

³ Beatrice Watson Parrent Fellow, Institute for Astronomy, University of Hawaii at Mānoa.

dances are typical. The star α Centauri A provides an excellent opportunity for comparison since it is a reasonable solar analog, having a temperature, gravity, and age quite similar to the Sun's. The Li abundance of α Cen A is known to be similar to (though a bit larger than) the Sun's (Chmielewski et al. 1992). Photographic data also suggest that the Be abundance of α Cen A is only slightly larger than the Sun's (Dravins & Hultqvist 1977). In this paper, we reexamine the Be abundance of α Cen A using new CCD data since some improvements are now possible. We take into account that the α Cen system is about 0.25 dex more metal-rich than the Sun. Both components of the Be II doublet are blended with other lines; we can take this into account by synthesizing spectra, taking advantage of improved line lists. We reexamine the solar Be abundance and address the important issue of whether or not it is depleted. We also examine, for the first time, the Be abundance of α Centauri B. Finally, we discuss implications for stellar structure and evolution.

2. OBSERVATIONS AND DATA REDUCTION

We observed the Be II 3130 Å region of the α Cen stars and the daytime sky in 1993 May 6 (UT) at the Cerro Tololo Inter-American Observatory (CTIO) 4 m telescope using the echelle spectrograph. This wavelength region contains the Be II resonance doublet with components at 3130.42 and 3131.07 Å. The measured resolution (from Th-Ar lamp spectra) is $R \sim 19000$ Å (~ 2.4 pixels) with a dispersion of ~ 0.068 Å pixel $^{-1}$ at 3131 Å. Standard IRAF routines were used for data reduction. Further details are presented in Deliyannis et al. (1996). The per pixel signal-to-noise ratio (S/N) values, determined from Poisson statistics in the Be II region, of the α Cen A and B spectra are 195 and 180, respectively. Since the effective S/N in our flat-field frame is comparable to these values, the effective S/N realized is somewhat lower—about 140.

3. ANALYSIS

Be abundances have been derived here by spectrum synthesis of the Be II 3130 Å resonance-line region using an updated version of the LTE analysis code MOOG (Sneden 1973) and the new Kurucz (1992) model atmosphere grids. The bluer, stronger Be II feature at 3130.42 Å is severely blended and will not be utilized here since this is exacerbated at our relatively low resolution. Instead, we focus on the weaker Be II feature at 3131.06 Å. This feature also appears to suffer from blending concerns that we discuss below.

3.1. Parameters

Chmielewski et al. (1992) have recently conducted a detailed analysis of α Cen A and B. We adopt the parameters that they determined: $T_{\text{eff}} = 5800 \pm 20$ K, $\log g = 4.31 \pm 0.02$ for α Cen A and $T_{\text{eff}} = 5325 \pm 50$ K, $\log g = 4.58 \pm 0.02$ for α Cen B. We adopt $[\text{Fe}/\text{H}] = +0.24 \pm 0.02$ for both stars based on their values of $+0.22 \pm 0.02$ and $+0.26 \pm 0.04$ for A and B, respectively; this value is also consistent with that, $+0.21$, found by Furenlid, Kurucz, & Meylan (1994), who used T_{eff} and $\log g$ -values nearly identical to ours. We use the guidance of Edvardsson et al. (1993) in adopting microturbulent velocities of 1.30 and 0.70 km s $^{-1}$ for α Cen A and B. The T_{eff} of α Cen B falls outside the range of calibration, so its microturbulence

value is a bit more uncertain. For the Be line strengths in question here, the derived abundance is insensitive to the adopted microturbulence (e.g., Boesgaard & King 1993). For the Sun, we adopt parameters of $T_{\text{eff}} = 5770$ K, $\log g = 4.44$, $[\text{M}/\text{H}] = 0.0$ (by definition), and a microturbulence of 1.10 km s $^{-1}$.

3.2. Line List Calibration

The 3130 Å spectral region, which contains the Be II resonance features we consider here, is rich with strong lines in solar-type stars. This results in substantial line absorption and a deficit of true continuum “windows.” Especially in the case of Population I stars, spectrum synthesis aids the determination of reliable Be abundances by reducing uncertainty in the continuum location and by accounting for possible blending features. Unfortunately, laboratory studies of the identification, precise wavelengths, and oscillator strengths of the many features in this spectral region are few in number.

We have taken atomic and molecular (mostly OH) identifications, wavelengths, excitation potentials, and $\log gf$ -values from the new Kurucz CD-ROM line lists. Oscillator strengths for the two Be II features, however, were taken from Wiese & Martin (1980). Our procedure was to alter the Kurucz gf -values in order to obtain a satisfactory fit to the Kurucz et al. (1984, hereafter K84) solar flux atlas, since our CTIO spectra are flux data. This exercise was greatly aided by MOOG, which returns a relative line-strength measure for every feature in the line list. This measure was first used to cull the list of the very weakest features; however, we retained features with line strengths even 5–6 orders of magnitude lower than typical values.

While this procedure has a degree of arbitrariness, it seems necessitated given the lack of empirical information. In cases of ambiguity, our philosophy was to adjust lines whose gf -values needed the least adjustment (i.e., believing that, on the whole, it seemed more reasonable to adjust gf -values by, e.g., factors of 5 rather than several orders of magnitude). In other cases of ambiguity, profile and depth information seemed to strongly favor one feature over another. In some cases, however, the choice of features to adjust is purely arbitrary. The resulting synthesis (*solid line*) for a Be abundance of $A(\text{Be}) \equiv 12 + \log [N(\text{Be})/N(\text{H})] = 1.12$, which proved to be the best fit to the red wing of the observed profile and as much of the base as possible, is shown versus the K84 solar atlas data (*filled squares*) in Figure 1a. We shall refer to this as our “canonical” solar Be abundance.

We note that, up to this point, we have not adjusted any features in the vicinity of the blue wing of the Be profile nor in the immediate vicinity of the Be II 3131.065 Å line itself, except for the CH λ 3131.058 feature. We reduced the $\log gf$ -value of this feature by adopting a lowered value kindly communicated by Ryan (1996), who has placed constraints on the oscillator strength by comparison of synthetic spectra and our high-resolution Keck I/HIRES Be data of stars having a large range in temperature, gravity, metallicity, and Be abundance. Even with these upper limits, the CH line strength is not totally negligible for detailed comparisons.

Excluding the region of the red Be II line, which we discuss next, the general agreement is good. Both this agreement and the few glaring discrepancies seem to be substantially similar to other modern synthesis analyses (e.g.,

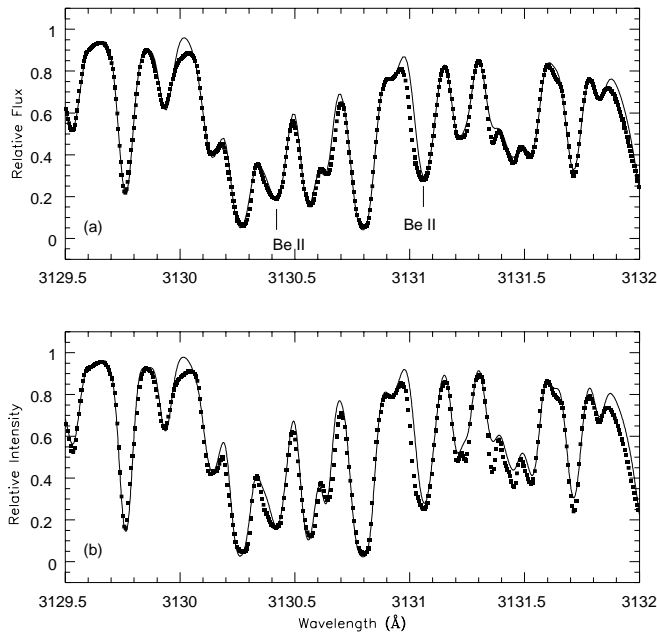


FIG. 1.—(a) LTE synthetic spectrum (solid line) with $A(\text{Be}) = 1.12$ vs. the K84 Solar Flux Atlas data (filled squares). The positions of the two Be II features are indicated. Deviation from otherwise reasonable agreement is seen just to the blue of the redder Be II feature. (b) LTE synthetic spectrum for $\mu = 1.0$ vs. the Delbouille et al. (1973) solar disk center atlas data. For the purposes of clarity, data points that intervene those shown have been excluded in the plots of both atlases.

Garcia Lopez, Rebolo, & Perez de Taoro 1995, hereafter GL95). We also find reasonable agreement between the syntheses and the corresponding GL95 spectra and syntheses of cool Hyades dwarfs, which should be similar to α Cen B. However, detailed comparison of syntheses and spectra of stars having a much larger range of T_{eff} , gravity, metallicity, and Be abundance will be required to reach fuller conclusions about uniqueness issues and the detailed adequacy of the line list.

One comparison that can be carried out at present, however, is that with solar disk center data, which are not affected by rotational broadening and might exhibit cleaner continuum windows. As such an additional check on the line list and the K84 continuum level, we performed a solar synthesis for disk center using our flux-calibrated line list. This is compared with the Delbouille, Neven, & Roland (1973, hereafter DNR73) disk center atlas data (kindly made available in electronic form by L. Delbouille and C. Servais) in Figure 1b. The overall agreement of the flux atlas-calibrated synthesis with the disk center data is very good. The few glaring discrepancies are the same ones seen in Figure 1a. Using the syntheses as a benchmark, a comparison of Figures 1a and 1b indicates that the adopted continuum levels of both atlases are very close to one another, but it may suggest that the K84 atlas continuum setting is slightly lower than that of DNR73. Whether this is a small genuine difference or a small difference in the syntheses (our benchmark) caused by errors of omission or commission in the atomic data, however, is not completely clear. In particular, both atlases suggest that the cleanest point in the remote Be II region is at ~ 3129.65 Å; thus, comparisons might be better carried out there. While not visible from Figure 1 because of the scale and finite data point size, the continuum levels differ slightly there also, but in the

opposite direction, i.e., the K84 atlas appears to have a higher continuum setting when the syntheses are used as a benchmark. Our conclusion is that the K84 and DNR73 continuum placements are consistent with one another. However, we cannot exclude the possibility that both placements are slightly but consistently in error.

3.3. Blending Features near the Red Be II Line

Using very high resolution spectra of the Sun taken at disk center ($\mu = 1.0$) and near the limb ($\mu = 0.2$), Chmielewski, Muller, & Brault (1975, hereafter CMB75) presented convincing evidence that there exists a significant contributor (centered near 3131.019 Å) to the red Be line blend. They treated this feature as a (fictitious) Ti II line. Others have also noted the existence of an interloping contributor (e.g., GL95 and Thorburn & Hobbs 1996). GL95 have treated (although not ascribed) this blending feature as the neighboring Mn I 3131.037 Å line by increasing its oscillator strength by 1.5 dex relative to the Kurucz value.

Figure 2a is a magnified version of Figure 1a around the red Be II feature. The rather poor fit of the synthesis to the observed feature depth, blue profile, and $\lambda 3130.97$ peak is clear. Figure 2b shows the same region of the spectrum, which has now been synthesized with enhancement of the Mn I $\lambda 3131.037$ log gf -value by 1.5 dex following GL95 (for all syntheses shown in Fig. 2, we have not altered our canonical solar Be abundance of 1.12 used in § 3.2). We find that the synthetic feature depth is already becoming too large, yet the blue profile is still not broad enough to match the data. Without enhancement of other features near 3131.00 Å, Mn I would appear to be too red if it is the sole

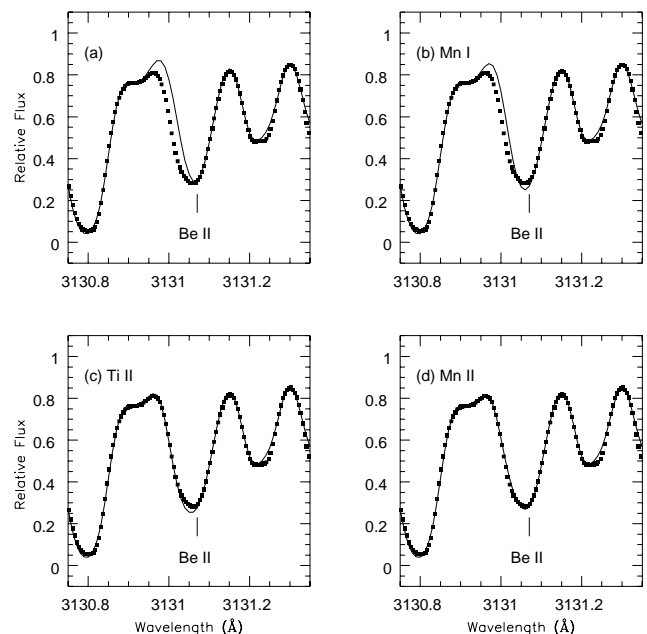


FIG. 2.—(a) A magnified version of Fig. 1a around the Be II 3131.06 Å region. A notable discrepancy between the synthesis (solid line) and the observational data (filled squares) is seen. (b) Synthesis with the Mn I $\lambda 3131.037$ feature's log gf -value enhanced by 1.5 dex. While the fit to the data is improved over (a), the line depth already appears to be too deep, and the blue profile would suggest that the Mn I line is not strong enough. (c) Synthesis with the fictitious Ti II 3131.019 Å line of CMB75. While the blue profile is fit well, the line depth is too large. (d) Synthesis with the Mn II 3131.015 Å line's log gf -value increased by 1.726 dex. The fit to the whole profile is very good, and it is perfect if the CH $\lambda 3131.058$ feature is discarded altogether.

significant blending feature. The same conclusion is reached about the CH $\lambda 3131.06$ feature.

Figure 2c shows the same region of the spectrum, which has now been synthesized adding CMB75's fictitious Ti II line and returning Mn I to its original Kurucz value. The Ti II gf -value was determined by requiring that CMB75's disk center equivalent width of 18 mÅ reproduce the Anders & Grevesse (1989, hereafter AG89) solar Ti abundance. The fit here is much improved over Figures 2a and 2b, although the synthetic line depth apparently is still too strong. If the line depth is matched (by reducing the gf -value), then the blue wing of the profile is noticeably discrepant. This might suggest that a single blending feature lies even slightly further to the blue.

Interestingly, the internal MOOG line-strength parameter indicates that the Mn II $\lambda 3131.015$ feature is somewhat stronger than the Mn I $\lambda 3131.037$ feature considered by GL95. Hence, to match the blue side of the 3131.06 Å profile, less enhancement would be needed for the Mn II line than would be needed for the Mn I line. Figure 2d shows a synthesis with the Ti II feature removed, the Mn I strength at the nominal Kurucz value, and the Mn II oscillator strength enhanced by 1.62 dex. It can be seen that the Mn II enhancement provides an excellent fit to the whole profile, although the reddest portion of the blue wing is not perfectly fit; perhaps not much significance can be attached to this given the various uncertainties. We also note that if the CH $\lambda 3131.058$ feature is discarded altogether, then the Mn II fit (with a log gf enhancement of 1.726 dex) is nearly perfect.

While a preliminary inspection of our Keck/HIRES Hyades giant spectra indicates a strong contribution by an unknown line near $\lambda \lesssim 3131.02$ Å, not inconsistent with the Mn II $\lambda 3131.015$ identification, a comparison of synthesized spectra, including this enhanced Mn II feature, with our data for Procyon (which has no detected Be) indicates that this feature is too strong, perhaps by a factor of 2. It is still possible that uncertainties in the line list (which not only affect the syntheses directly, but also indirectly via, e.g., estimation of the appropriate macroturbulence/instrumental profile/rotation convolution to be applied) are responsible for at least part of this discrepancy. Another alternative might be that there is an error in the Mn I $\lambda 3131.037$ wavelength of ~ 0.02 Å. An error of this magnitude is not unreasonable. A comparison of syntheses with the enhanced Mn I with our Procyon data show quite good agreement with the line depths and morphology of the profile of the red wing. However, as for the Sun, the synthetic blue wing is elevated relative to the data. A small wavelength shift could rectify this, although again other uncertainties in the line list cannot be excluded as the cause at this time.

We also investigated the possibility of a feature near 3131.00 Å working in tandem with the Mn I feature at 3131.04 Å to produce the blending. There is an OH feature at 3130.997 Å in the Kurucz line list. Such a combination might produce a strong feature near ~ 3131.02 Å in the cool, low-gravity Hyades giants. A partial contribution from Mn I might also mitigate the constraint noted by Thorburn & Hobbs (1996), who found that treating the unknown contributor(s) as a single OH line results in a feature that is too strong in halo stars. Unfortunately, so far we have been unable to locate any empirical confirmation of an OH feature at this wavelength, and, more importantly, we find that no combination of gf -value adjustments to the

Mn I and OH lines provides a satisfactory fit to the solar spectrum. Further comparisons of syntheses and spectra of stars having a wider range of parameters and abundances, additional line list refinements, and eventual experimental efforts are clearly needed to securely identify the contaminating line(s) in the Be II 3131.06 Å region. At this time, however, we are not convinced a single feature as red as ~ 3131.04 Å is the most plausible solution.

3.4. Relative ${}^9\text{Be}$ Abundance of α Cen A

To derive the Be abundances of α Cen A and B self-consistently relative to the Sun, we will use our CTIO spectra of all three stars.

Figure 3a shows our CTIO solar spectrum (*filled squares*), adjusted to rest wavelength, and our LTE Mn II $\lambda 3131.015$ -enhanced syntheses (*solid, dashed, and dotted lines*; convolved with a Gaussian to mimic the instrumental resolution, rotational profile, and macroturbulence) for three different Be abundances: $A(\text{Be}) = 1.31, 1.11,$ and 0.91 . The favored abundance, 1.11 ± 0.08 , was the value that minimized the χ^2 value for the few points around the red Be feature. The agreement with our canonical value of 1.12 (§ 3.2) from the higher resolution, higher S/N Kurucz atlas is encouraging. The quoted uncertainty was determined by noting abundance differences that resulted in χ^2 values different from the best-fit value at the 1σ confidence level according to an ordinary F -test.

Figure 3b shows our CTIO spectrum, adjusted to rest wavelength, of α Cen A (*filled squares*) versus Mn II-enhanced LTE syntheses (*solid, dashed, and dotted lines*) using a model atmosphere interpolated from the Kurucz (1992, hereafter K92) $[M/H] = +0.2$ grid. In the syntheses, all metal abundances were enhanced by $+0.24$ over the nominal solar values except for the abundances of the odd

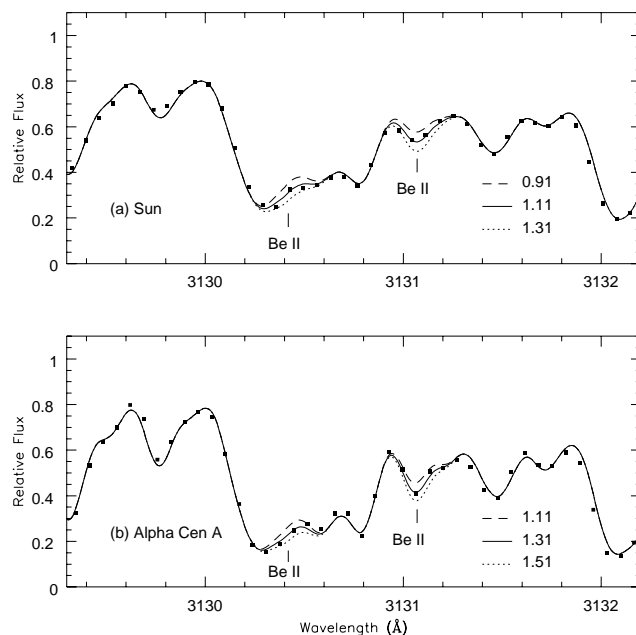


FIG. 3.—(a) Our CTIO daytime sky solar spectrum (*filled squares*) vs. LTE syntheses (smoothed with a Gaussian to simulate the instrumental resolution, rotational profile, and macroturbulence) with three different Be abundances, $A(\text{Be}) = 0.91, 1.11$ (the best-fit value), and 1.31 . (b) Our CTIO spectrum of α Cen A (*filled squares*) vs. syntheses (again Gaussian smoothed) with abundances $1.11, 1.31,$ and 1.51 .

elements Na, Sc, Mn, and Cu. These elements were found to have enhanced abundances ($[X/Fe]$) in α Cen A by Furenlid et al. (1994). Whether this is a genuine difference or the result of neglect of hyperfine structure remains unclear, however. Our best-fit Be abundance is $A(\text{Be}) = 1.31 \pm 0.10$.

Our derived relative Be abundance is then $[\text{Be}/\text{H}] = +0.20 \pm 0.15$, where the uncertainty is the 1σ confidence level random error estimate. This was obtained by combining the fitting uncertainties, random uncertainties in the continuum placement (which amount to ~ 0.03 dex for both objects), and uncertainties in the α Cen A parameters. Since we are interested here in the relative Be abundance of α Cen A, we have ignored systematic sources of error due to Be gf -value uncertainties, scattered light, model atmosphere deficiencies, etc.

Other potential sources of systematic error include adoption of the K84 atlas and its continuum normalization in the calibration of the line list. However, the *differential* effect of this on the relative abundances is small. CMB75 used the peak at ~ 3129.7 Å as continuum; clearly this provides a lower bound to the continuum. Using this continuum level and scaling approximate Be line strengths, the solar Be abundance is lowered just slightly more than is that of α Cen A, and $[\text{Be}/\text{H}]$ increases by ≤ 0.05 dex.

Another possible systematic error source is the Mn abundance. If a lower Mn abundance, consistent with the even-numbered metals, is adopted for α Cen A, we derive a $[\text{Be}/\text{H}]$ value larger by ~ 0.05 dex. Thus, besides the random $[\text{Be}/\text{H}]$ errors of ± 0.15 dex, systematic errors of order ~ 0.1 dex are also possible. We also note that, to within a few hundredths of a dex, the same $[\text{Be}/\text{H}]$ value is found using the Mn I $\lambda 3131.037$ -enhanced line list. However, the fit to the observed data is not as good. The same effect noted in the comparisons using the high-quality K84 data is, perhaps encouragingly, seen even in our low-resolution, lower S/N spectra. Namely, the red wings of the synthetic Be II blend profile are too strong while the core and blue wings are too shallow relative to the data.

To summarize, $[\text{Be}/\text{H}] = +0.20 \pm 0.15$ (random) ± 0.10 (systematic).

3.5. ^9Be Abundance Upper Limits on α Cen B

GL95 have discussed the uncertainties in deriving Be abundances in metal-rich cool dwarfs. As they note, better atomic and molecular data and high-quality spectra are needed to derive secure Be abundances in these stars. Blending is particularly problematic at our low resolution. Since, however, there are no previous published Be abundances for α Cen B, we have attempted to use our low-resolution spectra and (certainly still incomplete) line list to place an upper limit.

Figure 4 shows our CTIO spectrum (*filled squares*), adjusted to rest wavelength, and LTE synthesis (*solid, dashed, dash-dotted, and dotted lines*) for abundances $A(\text{Be}) = -0.04, 0.86, 1.16,$ and 1.46 . The top panel is the synthesis utilizing the enhanced Mn II $\lambda 3131.015$ gf -value. The bottom panel shows the synthesis for the Mn I $\lambda 3131.037$ gf -value. The general agreement of the synthesis with the observed spectra for this cool star seems reasonable, although not as good as for the Sun and α Cen A. Notable discrepancies are seen at 3130.2, 3130.7, and 3132.1 Å. Inspection of both the blue Be II feature (which itself undoubtedly has nonnegligible blending uncertainties) and the red Be II feature in Figures 4a and 4b suggests that

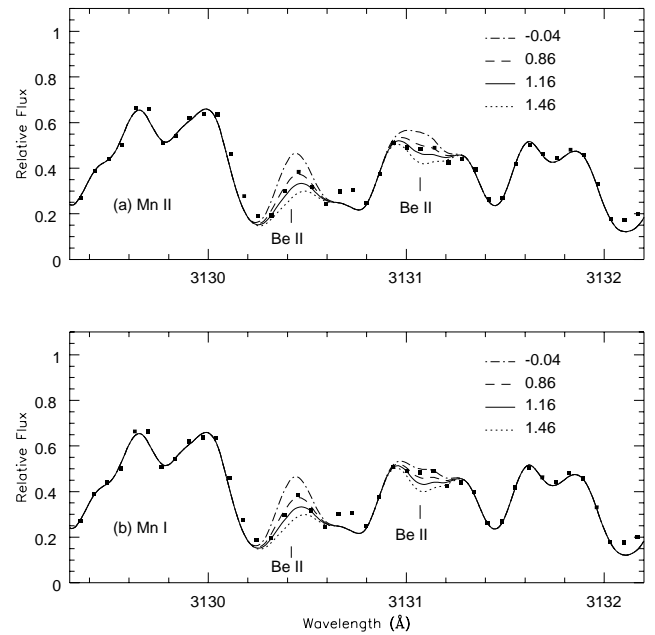


FIG. 4.—(a) CTIO spectrum of α Cen B (*filled squares*) vs. Mn II $\lambda 3131.015$ gf -enhanced syntheses (*solid, dashed, dash-dotted, and dotted lines*) with abundances $A(\text{Be}) = -0.04, 0.86, 1.16,$ and 1.46 . (b) Same as (a), except the syntheses were conducted with the Mn I $\lambda 3131.037$ gf -enhanced line list.

$[\text{Be}/\text{H}] \lesssim +0.05$. While, at face value, this Be abundance is 0.15 dex lower than that derived for α Cen A, the uncertainties in the latter value (to say nothing of those in the former) are large enough that the difference is not significant.

We also conducted syntheses with the Mn I $\lambda 3131.037$ feature shifted blueward by 0.020 Å (as proposed above). The morphology of the red Be II blend synthesis is considerably closer to the observations (i.e., noticeably flatter than the synthetic profiles shown in Fig. 4), perhaps again favoring a wavelength this blue for a single unidentified blending feature. These syntheses suggest a Be abundance about a factor of 2 lower than the above limit. However, the Be abundances inferred from the red and blue Be II features are discrepant. Although this could merely be a result of blending uncertainties in the blue Be II line region, we prefer to retain the more conservative value above. We have also considered the effect of lowering the assumed $[\text{Mn}/\text{H}]$ ratio from $+0.36$ to the nominal value assumed for the other (even) elements, $+0.24$. For the nominal wavelength Mn I and Mn II gf -enhanced cases, we find that the sloping shape of the red Be II blend is exacerbated relative to that seen in Figure 4. For the adjusted Mn I wavelength case, $[\text{Mn}/\text{H}] = +0.24$ may be preferred, but little significance can be attached to this.

4. DISCUSSION

4.1. Absolute Solar ^9Be Abundance

4.1.1. Importance of Beryllium

A comparison of several open clusters of different ages shows that in solar-type stars (e.g., G stars), progressively older clusters have progressively lower Li abundances (Boesgaard 1991; Soderblom et al. 1993; Ryan & Deliyannis 1995). The simplest interpretation is that this reflects

Li depletion with age, which presents a serious problem for standard stellar models (which ignore possible effects due to rotation, microscopic diffusion, magnetic fields, and mass loss).⁴ Standard models generally deplete Li only during the pre-main sequence since the surface convection zone becomes shallower as models evolve to the turnoff. Thus, whereas standard models might be able to explain the mean Li depletion in G stars in a cluster the age of the Pleiades, it is not clear that they can explain the more severely depleted older clusters.

One possible solution is to modify the “standard” physics, e.g., extending the convection zone by invoking convective overshoot or a larger mixing length. But such a solution has drawbacks: (1) a deeper solar convection zone would be in conflict with helioseismology, and (2) while more Li depletion might be possible, it would still take place only during the pre-main sequence; so while the Li in G stars of one cluster might be explained, Li in other clusters of different ages would be in contradiction. These arguments and others (particularly the existence of less Li-depleted, short-period, tidally locked binaries in a variety of stellar populations; Ryan & Deliyannis 1995) point to the need to consider additional physics other than what is included in the standard models.

A common feature of standard models and the convection zone modifications discussed above is that Li depletion occurs at the base of the surface convection zone when the temperature (and density) are high enough. Another common feature is that Be, which requires a higher temperature for destruction, is *not* destroyed in solar models or in any stellar model that contains observable amounts of Li. Since the convection zone mixes on an extremely short timescale compared with the evolutionary timescale, material at the surface spends a significant fraction of its time at the hot base of the convection zone. Thus, even a small amount of nuclear Be destruction implies *many* orders of magnitude of Li destruction.

A depletion of solar Be would suggest an alternate solution. A small amount (factor of ~ 2) of Be depletion would be possible, even though solar Li is depleted by only a factor of ~ 200 (not many orders of magnitude), *if* slow (i.e., a timescale comparable to the evolutionary timescale) mixing occurred below the surface convection zone. Such mixing would then be more akin to a dilution process in which Be could be diluted while Li was still present. Just such a scenario results from the Yale approach to modeling stellar

⁴ This conclusion seems to rest, in part anyway, on *assumed* scaling of elemental abundances, which provide the needed model input surface and interior opacities important to the Li depletion calculations, with Fe. Swenson et al. (1994) have suggested that opacity uncertainties may be able to reconcile standard model calculations with the observed gross morphology of Li depletion in the Hyades. Investigating whether plausible opacity adjustments can explain Li abundances in other (older) clusters requires detailed abundances of specific elements such as O, Mg, and Ne. Unfortunately, these observational data are lacking. For standard stellar models to be able to account for the observed Li-age relation, it would be necessary for progressively older clusters to be progressively more *enriched* in at least some elements; the results of Friel & Janes (1993) may be of some interest in this regard. It will also be necessary to investigate the effect of increased metallicity on the surface opacities (which are easily underestimated) in standard models, which can result in cooler effective temperatures for the models. It may turn out that this effect dominates over any increased Li depletion in a model of a given *mass*, so that instead of metal-rich Li isochrones being lower, they end up being cooler (i.e., higher) than solar metallicity ones, or perhaps quite similar if the effects effectively cancel each other out.

rotation (Endal & Sofia 1978; Pinsonneault et al. 1989; Pinsonneault, Kawaler, & Demarque 1990). The latter studies found that, for calibrated solar models with Li depleted by ~ 2.2 dex, Be depletion is about 0.3–0.5 dex (~ 0.5 dex of Li depletion, but none of the Be depletion, occurs during the pre-main sequence at the base of the surface convection zone, in apparent agreement with Pleiades Li data). The more recent models of Deliyannis & Pinsonneault (1993), which include various improvements in the input physics (e.g., use of the Los Alamos Opacity Library opacities; Huebner et al. 1977; Huebner 1978), have slightly less Be depletion. Since the Yale rotational models have wide-ranging implications for astronomy (e.g., the review by Deliyannis 1995), it is important to ascertain whether or not the solar Be abundance is depleted and by how much.

4.1.2. Solar Photospheric Be Abundance

In order to derive the likely range of the solar photospheric Be abundance, we utilize the very high resolution and S/N data of the K84 flux and the DNR73 disk center atlases. We begin with our canonical Be abundance of 1.12 (§ 3.2) and first consider various uncertainties that could raise this value. In deriving a maximum Be abundance, we use the DNR73 atlas because of its apparently (slightly) higher continuum normalization. First, we note that the higher continuum setting of DNR73 (or K84) relative to the CMB75 continuum setting is a conservative assumption in this sense. We have also removed the CH 3131.06 Å line from consideration as a further conservative assumption (its inclusion would lower our derived Be abundances by ~ 0.04 dex) and kept the nearby Mn I and Mn II oscillator strengths at their nominal Kurucz values. We then performed LTE synthesis using MOOG and the K92 solar model atmosphere. Our maximum abundance [$A(\text{Be}) = 1.25$] was that for which the synthetic Be II line core departs below the observed Be-blend profile.

Uncertainties in the *gf*-value ($\pm 10\%$) lead to abundance differences of ± 0.04 dex. Given the above conservative assumptions and the fact that the red wing (mostly due to Be) departs from the observed profile somewhat before the line core (which lacks inclusion of the important blending contributor), the abundance derived in this fashion, and augmented by 0.04 dex for the *gf* uncertainty [yielding $A(\text{Be}) = 1.29$], should be a secure upper limit to the Be abundance given the various explicit assumptions (continuum setting, model atmospheres, LTE assumption, choice of code) in the analysis. These assumptions must be considered further.

The use of the DNR73 data carries with it its specific continuum normalization, and it must be borne in mind that our maximum value assumes explicitly that this is correct. While it remains difficult to definitively exclude higher continuum normalizations, this is at least a conservative assumption with respect to the CMB75 and perhaps the K84 data. We have compared abundances derived from the K92 model atmospheres with those derived using other atmospheres. Comparisons of possible interest are those using the Harvard-Smithsonian Reference Atmosphere (Gingerich et al. 1971) the Holweger-Muller (1974), and the newer generation MARCS (Gustafsson et al. 1975) atmospheres. The derived K92-based Be abundance is larger than these other cases by 0.03, 0.03, and 0.08 dex. Since the Holweger & Muller (1974) model is still widely regarded as

the superior model atmosphere for deriving absolute solar photospheric abundances, we adopt the Be abundance it would yield [$A(\text{Be}) = 1.26$].

Kiselman & Carlsson (1995) and Garcia Lopez, Severino, & Gomez (1995) have investigated non-LTE effects on abundances derived from the red Be II feature. They find the effects to be very small (~ 0.01 dex) for the Sun, although this does not mean the lines are formed in LTE. Due to the nature of the problem, non-LTE corrections depend on the details of the model atmosphere. Therefore, non-LTE corrections derived using a particular atmosphere may not be strictly applicable to abundances derived using other atmospheres. While the above authors base their non-LTE calculation on OSMARCS and MARCS models, and while we rely on other models for our best estimates, one expects that the solar non-LTE corrections should be the same to first order.

We have also taken a cursory look at code-dependent differences on the Be abundance. We compared abundances derived for various Be II $\lambda 3131.06$ equivalent widths using the MOOG and RAI10 packages. There appear to be small but nonnegligible differences, but the cause is unclear. A variety of comparisons indicate that these differences are primarily a function of T_{eff} ; only small abundance differences (0.02–0.03 dex) are seen over an equivalent width range 5–110 mÅ. At 6500 K, the typical RAI10–MOOG Be abundance difference for any equivalent width is only 0.01 dex. But at solar T_{eff} , the difference is 0.07–0.08 dex. The difference climbs to ~ 0.12 dex at 5250 K. Using the SYNTHE code (Kurucz & Avrett 1981), Thorburn & Hobbs (1996) determined Be abundances in six halo stars. Five of these stars were included in the study of Boesgaard & King (1993), who used the RAI10 abundance code. Thorburn & Hobbs (1996) noted systematic differences between their abundances and those of Boesgaard & King (1993), and ascribed these to differences in stellar parameters and analysis approach (spectrum synthesis vs. equivalent width measurements). A close comparison, facilitated by the kind cooperation of J. Thorburn, indicates that small analysis code (or implementation thereof) dependent differences also play a role. The T_{eff} -dependent differences between MOOG and RAI10 are nearly identical to those between SYNTHE and RAI10, perhaps suggesting the latter as the responsible culprit. We thus retain our MOOG-based upper bound of $A(\text{Be}) = 1.26$.

A minimum photospheric Be abundance was estimated by comparison of spectrum synthesis with the K84 flux atlas data, which possibly has a lower continuum setting than the DNR73 disk center data. We used the Mn I gf -enhanced line list, reincorporating the CH $\lambda 3131.06$ feature to be conservative. The Be abundance was reduced until the synthetic profile departed from the core and red wing of the K84 Be II $\lambda 3131.06$ blend. This value [$A(\text{Be}) = 0.99$] was further reduced by 0.04 dex to account for possible uncertainties in the Be gf -value, and lowered a further 0.03 dex to account for the systematic difference in preferring the Holweger-Muller atmosphere. This leaves us with a lower abundance bound of $A(\text{Be}) \geq 0.92$. Our final conservatively estimated probable range for the solar photospheric Be abundance is thus $0.92 \leq A(\text{Be}) \leq 1.26$. We find an extreme range, determined by stretching the noted atmosphere and code uncertainties to their fullest in the relevant direction and by assuming the continuum level of CMB75 in deriving a minimum bound, of $0.80 \leq A(\text{Be}) \leq 1.37$.

4.1.3. Implications

Our probable range for the solar photospheric Be abundance, $A(\text{Be}) = 0.92\text{--}1.26$, which considers the various sources of systematic errors discussed in the preceding subsection, suggests that Be is depleted relative to the AG89 meteoritic value (1.42 ± 0.04) by 0.16–0.50 dex. Such a depletion would strongly contradict the prediction from standard models that there should be no depletion of Be in the Sun, but it is in quantitative agreement with the Yale models that include rotationally induced mixing (§ 4.1.1). The confidence of this result depends here not only on the reliability of the solar atlas data and possible systematic differences in other families of atmospheres and abundance codes that we have not investigated, but also on the reliability of the meteoritic abundance, which we now address.

The AG89 meteoritic abundances are given on a Si-based scale, whereas photospheric abundances are given relative to hydrogen. In principle, the two scales may have systematic differences. However, AG89 find that “the nominal uncertainty in coupling the two scales now is only $\pm 5\%$.” Indeed, a comparison of the photospheric and the meteoritic abundances they present shows that the vast majority of elements agree to within the stated errors. Of those that disagree, proposed subsequent revisions in the photospheric abundances of some bring them into agreement. It would seem that scale differences are not the source of the difference between photospheric and meteoritic Be. AG89 note that three studies employing different techniques produced similar meteoritic Be abundances, strengthening the conclusion of a difference between photospheric and meteoritic Be due to solar depletion.

As discussed above, nuclear physics dictates that *any* Be destruction (at the base of the surface convection zone) in standard models would imply Li destruction by many orders of magnitude. However, the detected solar photospheric Li abundance is in stark contrast to this expectation. If solar Be is indeed depleted, it would thus provide strong evidence that slow mixing has occurred in the Sun, and would support the Yale rotational models. Such evidence would join other striking predictions of the Yale models that seem to be realized: the Population I mid-F star Li gap; the higher-than-average Li content of short-period binaries; the depletion of the Li peak (analogous to the halo Li plateau) in the old open cluster M67; the progressively lower Li with age in open clusters and the Sun and solar analogs (e.g., α Cen A, 16 Cyg A, 16 Cyg B); the short (relative to rigid rotation) rotational periods in subgiants; and the rapidly rotating horizontal branch stars (see, e.g., Deliyannis 1995 and Sofia, Pinsonneault, & Deliyannis 1991 for reviews).

An especially relevant prediction (Deliyannis & Pinsonneault 1993) is the observed depletion of Be in late F stars, which have depleted, but detectable Li (Stephens et al. 1996). Essentially the same mechanism (slow mixing in the outer layers due primarily to secular shear) in the Yale models can account for this as for a solar Be/Li depletion, but with an important difference: in late-F star models, the main-sequence convection zone has negligible depth compared with the Li and Be preservation regions. As a result, slow mixing accomplishes the entire Li/Be depletion (via dilution as described above), which yields more Be depletion at a given Li depletion factor. Hence, late F stars (e.g., 110 Her) can have Be depleted by about a factor of 5–10,

but Li depleted by only a factor of 100. In contrast, the convection zone occupies a significant fraction of the Li preservation region in models of cooler stars (e.g., the Sun). Since convection accomplishes the mixing in the region where it occurs, rotational mixing influences the layers just below the convection zone more in cooler stars than in the comparable region in F stars. Thus, at a given Li depletion factor (e.g., 100), there will be less Be depletion (e.g., factor of 2), as seems to be the case for the Sun. The agreement between the model predictions and the quantitative difference between the Li/Be ratio in these F stars and cool stars, like the Sun, lend strong support to the models.

Finally, we wish to point out the cosmologically important Yale model prediction that the halo Li plateau would be depleted from its initial value by roughly a factor of 10 (Deliyannis 1990; Pinsonneault, Deliyannis, & Demarque 1992; Chaboyer & Demarque 1994). The inferred high value of the primordial Li abundance has implications for standard and inhomogeneous big bang nucleosynthesis and for dark matter (e.g., Deliyannis et al. 1996 and references therein).

4.2. Implications of the Li and Be Abundances of α Cen A and B

In spite of the fact that α Cen A is nearly a factor of 2 more metal-rich in many elements than the Sun (Chmielewski et al. 1992; Furenlid et al. 1994), its Li abundance is higher, not lower, than the Sun's by about a factor of 2 (at the same T_{eff} , this abundance is still more than 1 dex lower than the Hyades and more than 1.5 dex lower than the Pleiades). If metal-rich standard models predict increased Li depletion with metallicity, then α Cen A contradicts this (*ceteris paribus*; see below) and points to the effects of an additional mechanism (such as rotationally induced mixing). Standard models of sufficiently high metallicity (and helium abundance) should be constructed, taking into account uncertainties and effects of surface opacities, to quantitatively investigate this.

One might wonder whether the initial Li abundance in α Cen A might have been higher, leading to a larger current abundance. If the Li depletion in α Cen A is to exceed that in the Sun as the result of "metallicity" differences, then its initial abundance would have had to have been greater than $A(\text{Li}) \sim 3.6$. While we cannot rule out such high initial values, the preponderance of the evidence suggests little enrichment from the meteoritic abundance of 3.30 some 4.5 Gyr ago. Young open clusters generally display maximum Li abundances between 3.0 and 3.3.

In contrast to Li, Be has been shown to increase in the halo (e.g., Ryan et al. 1990). The situation in the Galactic disk (e.g., Boesgaard & King 1993) is much less clear since there is considerable dispersion, some of which may be due to stellar depletion and some of which may be due to Galactic production, in the Be abundances. It is certainly possible that α Cen A and B formed with a higher initial Be abundance than the Sun. It is thus difficult to ascertain whether a possibly higher Be abundance in α Cen A reflects more or less Be depletion than in the Sun, or any Be depletion at all.

Comparison of the Be abundances of α Cen A and B is of interest, since they presumably had the same initial abundance. While our upper limit for α Cen B of $[\text{Be}/\text{H}] \lesssim +0.05$ is not inconsistent with our abundance for α Cen A (+0.20) given the uncertainties, Figure 4 shows that our data could indicate an even larger (~ 0.3 dex) difference.

Higher resolution data of both stars and further refinements in the line list are needed to better constrain any real abundance difference. Such efforts are of importance since the standard models of Pinsonneault et al. (1990) indicate that only much cooler stars ($T_{\text{eff}} \sim 4000$ K) with much deeper convection zones deplete Be. Thus, if α Cen B (at 5300 K) is depleted relative to α Cen A, this would strongly suggest the action of additional mixing mechanisms. Slow rotationally induced mixing can accommodate a higher, lower, or similar abundance in α Cen B as in α Cen A (depending on the details of how the mixing occurs), whereas standard models predict the same undepleted Be abundance for both stars.

5. SUMMARY AND CONCLUSIONS

We have presented high S/N and moderately high resolution spectroscopy of the Be II 3131 Å region for α Cen A and B. Abundances relative to the Sun have been derived self-consistently via LTE spectrum synthesis. In considering the unidentified blending feature(s) that perturbs the Be II 3131.065 Å line, we believe that a feature (perhaps most likely a neutral or molecular species) located at $\lambda \lesssim 3131.02$ Å is most plausible.

Our derived Be abundance for α Cen A is $[\text{Be}/\text{H}] = +0.20$, with a 1σ level random uncertainty estimate of ± 0.15 dex. Systematic errors at the level of ~ 0.1 dex are also possible. For the significantly cooler and more severely blended α Cen B, we find $[\text{Be}/\text{H}] \lesssim +0.05$. While there is some indication that the abundance could be even lower, we prefer to retain this more conservative estimate, which cannot be said to be significantly different from the abundance of α Cen A given the uncertainties.

The analysis of high-quality solar atlas data and the consideration of various uncertainties (e.g., *gf*-values, continuum location, non-LTE effects, model atmosphere differences, code-dependent differences) lead us to conclude conservatively that the probable range in the current solar photospheric Be depletion is 0.16–0.50 dex relative to the initial (meteoritic) value. If true, this would strongly suggest the action of additional mixing mechanisms since standard stellar models predict no Be depletion for the Sun. In particular, a slow-mixing mechanism (such as rotationally induced mixing) may be indicated to account for the fact that the depletion of solar Li is only ~ 2 orders of magnitude. The Sun, then, can be seen as a cooler analogy to the small population of late F stars that demonstrate significantly depleted Be but yet retain observable Li. The Yale rotational stellar models (Pinsonneault et al. 1990; Deliyannis & Pinsonneault 1993; Deliyannis 1995) are able to account for the solar and F star Li/Be ratios as well as a large number of other phenomena.

A genuine difference in the Be abundances of α Cen A and B would also strongly suggest inclusion of nonstandard physics in stellar models. Standard models predict that Be depletion occurs only in much cooler ($T_{\text{eff}} \sim 4000$ K) stars than α Cen B. Higher resolution spectra and future line list refinements will be necessary for (but may not guarantee) more secure derivation of the relative Be abundances of α Cen A and B.

Finally, we note that the photospheric Li and Be abundances of the Sun and the solar analogs α Cen A, 16 Cyg A, and 16 Cyg B are substantially similar. Of the solar Li depletion by a factor of 200, roughly a factor of 5 can be accounted for by standard solar models, leaving roughly

another factor of 40 unexplained. Thus, while there is, e.g., a factor of ~ 2 difference in the Li abundances of the Sun and α Cen A, this difference is much smaller than the unexplained factor of 40. Since all four of the above solar-type stars have very low Li and similar Be, excluding the Sun as an isolated “oddball” (as is done in other contexts, e.g., Galactic chemical evolution) seems an unlikely solution to the decades-old solar Li abundance problem.

J. R. K. and C. P. D. are supported by NASA through grants HF-1046.01-93A and HF-1042.01-93A from the Space Telescope Science Institute, which is operated by the Association of Universities for Research in Astronomy, Inc.,

under NASA contract NAS5-26555. We would also like to express our sincere thanks to the Eberly Foundation of the Pennsylvania State University for financial support of our CTIO observing run. We also are grateful to the CTIO TAC for the allotment of telescope time, and to the CTIO staff and telescope operators for their usual competent assistance. Further financial support was provided by NSF grant AST 90-16778 to A. M. B., and by the University of Hawaii Foundation to C. P. D. We thank D. Duncan for helpful discussions during the course of this work. This research has made use of the SIMBAD database, operated at CDS, Strasbourg, France.

REFERENCES

- Anders, E., & Grevesse, N. 1989, *Geochim. Cosmochim. Acta*, 53, 197 (AG89)
- Bahcall, J. N., & Pinsonneault, M. H. 1992, *Rev. Mod. Phys.*, 64, 885
- Boesgaard, A. M. 1991, *ApJ*, 370, L95
- Boesgaard, A. M., & King, J. R. 1993, *AJ*, 106, 2309
- Chaboyer, B., & Demarque, P. 1994, *ApJ*, 433, 510
- Chaboyer, B., Demarque, P., & Pinsonneault, M. H. 1995, *ApJ*, 441, 865
- Chmielewski, Y., Friel, E., Cayrel de Strobel, G., & Bentolila, C. 1992, *A&A*, 263, 219
- Chmielewski, Y., Muller, E. A., & Brault, J. W. 1975, *A&A*, 42, 37 (CMB75)
- Christensen-Dalsgaard, J., Gough, D. O., & Thompson, M. J. 1991, *ApJ*, 378, 413
- Delbouille, L., Neven, L., & Roland, G. 1973, *Photometric Atlas of the Solar Spectrum from λ 3000 to λ 10000* (Liège: Inst. Astrophys. Univ. Liège) (DNR73)
- Deliyannis, C. P. 1990, Ph.D. thesis, Yale Univ.
- . 1995, in *The Light Element Abundances*, ed. P. Crane (Berlin: Springer), 395
- Deliyannis, C. P., Boesgaard, A. M., King, J. R., & Duncan, D. K. 1996, *AJ*, submitted
- Deliyannis, C. P., & Pinsonneault, M. H. 1993, in *ASP Conf. Ser. 137, Inside the Stars*, ed. W. W. Weiss & A. Baglin (San Francisco: ASP), 174
- Dravins, D., & Hultqvist, L. 1977, *A&A*, 55, 463
- Edvardsson, B., Andersen, J., Gustafsson, B., Lambert, D. L., Nissen, P. E., & Tomkin, J. 1993, *A&A*, 275, 101
- Endal, A. S., & Sofia, S. 1978, *ApJ*, 220, 279
- Friel, E. D., & Janes, K. A. 1993, *A&A*, 267, 75
- Furenlid, I., Kurucz, R. L., & Meylan, T. 1994, in *ASP Conf. Ser. 64, Cool Stars, Stellar Systems, and the Sun*, ed. J.-P. Caillault (San Francisco: ASP), 560
- Garcia Lopez, R. J., Rebolo, R., & Perez de Taoro, M. R. 1995, *A&A*, 302, 184 (GL95)
- Garcia Lopez, R. J., Severino, G., & Gomez, M. T. 1995, *A&A*, 297, 787
- Gingerich, O., Noyes, R., Kalkofen, W., & Cuny, Y. 1971, *Sol. Phys.*, 18, 347
- Gustafsson, B., Bell, R. A., Eriksson, K., & Nordlund, Å. 1975, *A&A*, 42, 407
- Holweger, H., & Muller, E. A. 1974, *Sol. Phys.*, 39, 19
- Huebner, W. F. 1978, in *Proc. Brookhaven Solar Neutrino Conference*, Vol. 1, ed. G. Friedlander (Publ. 50879; Long Island, NY: BNL), 107
- Huebner, W. F., Merts, A. L., Magee, N. H., & Argo, M. F. 1977, *Los Alamos Scientific Lab. Rep. LA-6760-M*.
- Kiselman, D., & Carlsson, M. 1995, in *The Light Element Abundances*, ed. P. Crane (Berlin: Springer), 372
- Kurucz, R. L. 1992, private communication (K92)
- Kurucz, R. L., & Avrett, E. M. 1981, *SAO Spec. Rep.* 391
- Kurucz, R. L., Furenlid, I., Brault, J., & Testerman, L. 1984, *NSO Atlas 1, Solar Flux Atlas from 296 to 1300 nm* (Tucson: NSO) (K84)
- Pinsonneault, M. H., Deliyannis, C. P., & Demarque, P. 1992, *ApJS*, 78, 179
- Pinsonneault, M. H., Kawaler, S. D., & Demarque, P. 1990, *ApJS*, 74, 501
- Pinsonneault, M. H., Kawaler, S. D., Sofia, S., & Demarque, P. 1989, *ApJ*, 338, 424
- Ryan, S. G. 1996, private communication
- Ryan, S. G., Bessell, M. S., Sutherland, R. S., & Norris, J. E. 1990, *ApJ*, 348, L57
- Ryan, S. G., & Deliyannis, C. P. 1995, *ApJ*, 453, 819
- Snedden, C. 1973, *ApJ*, 184, 839
- Soderblom, D. R., Pilachowski, C. A., Fedele, S. B., & Jones, B. F. 1993, *AJ*, 105, 2299
- Sofia, S., Pinsonneault, M. H., & Deliyannis, C. P. 1991, in *NATO Adv. Res. Workshop: Angular Momentum Evolution of Young Stars*, ed. S. Catalano & J. R. Stauffer (Dordrecht: Kluwer), 333
- Stephens, A., Boesgaard, A. M., Deliyannis, C. P., & King, J. K. 1996, in preparation
- Swenson, F. J., Faulkner, J., Iglesias, C. A., Rogers, F. J., & Alexander, D. R. 1994, *ApJ*, 422, L79
- Thorburn, J. A., & Hobbs, L. M. 1996, *AJ*, 111, 2106
- Wiese, W. L., & Martin, G. A. 1980, *NBS Monograph 68* (Washington, DC: GPO)